



BET inhibitors reduce cell size and induce reversible cell cycle arrest in AML

Susu Zhang¹ | Yue Zhao¹ | Tiffany M. Heaster² | Melissa A. Fischer³ | Kristy R. Stengel¹ | Xiaofan Zhou⁴ | Haley Ramsey³ | Ming-Ming Zhou⁵ | Michael R. Savona^{3,6} | Melissa C. Skala² | Scott W. Hiebert^{1,6}

¹Department of Biochemistry, Vanderbilt University School of Medicine, Nashville, Tennessee

²Department of Biomedical Engineering, Morgridge Institute for Research, University of Wisconsin–Madison, Madison, Wisconsin

³Department of Medicine, Vanderbilt University School of Medicine, Nashville, Tennessee

⁴Department of Biological Sciences, Vanderbilt University School of Medicine, Nashville, Tennessee

⁵Department of Pharmacological Sciences, Icahn School of Medicine at Mount Sinai, New York, New York

⁶Vanderbilt-Ingram Cancer Center, Vanderbilt University School of Medicine, Nashville, Tennessee

Correspondence

Scott W. Hiebert, Department of Biochemistry, Vanderbilt University School of Medicine, 512 Preston Research Building, 2220 Pierce Ave, Nashville 37232, Tennessee.
Email scott.hiebert@vanderbilt.edu

Funding information

National Cancer Institute, Grant/Award Numbers: R01CA64140, R01CA178030, R01CA164605, 5 T32 CA009582-31; Vanderbilt Digestive Disease Research Center, Grant/Award Number: NIDDK P30DK58404; Vanderbilt-Ingram Cancer Center, Grant/Award Number: NCI P30CA68485; American Cancer Society, Grant/Award Number: PF-13-303-01-DMC; National Center for Research Resources, Grant/Award Number: UL1 RR024975-01; National Center for Advancing Translational Sciences, Grant/Award Number: 2 UL1 TR000445-06

Abstract

Inhibitors of the bromodomain and extraterminal domain family (BETi) offer a new approach to treat hematological malignancies, with leukemias containing mixed lineage leukemia rearrangements being especially sensitive due to a reliance on the regulation of transcription elongation. We explored the mechanism of action of BETi in cells expressing the t(8;21), and show that these compounds reduced the size of acute myeloid leukemia cells, triggered a rapid but reversible G₀/G₁ arrest, and with time, cause cell death. Meta-analysis of PRO-seq data identified ribosomal genes, which are regulated by MYC, were downregulated within 3 hours of addition of the BETi. This reduction of MYC regulated metabolic genes coincided with the loss of mitochondrial respiration and large reductions in the glycolytic rate. In addition, gene expression analysis showed that transcription of *BCL2* was rapidly affected by BETi but this did not cause dramatic increases in cell death. Cell cycle arrest, lowered metabolic activity, and reduced *BCL2* levels suggested that a second compound was needed to push these cells over the apoptotic threshold. Indeed, low doses of the *BCL2* inhibitor, venetoclax, in combination with the BETi was a potent combination in t(8;21) containing cells. Thus, BET inhibitors that affect MYC and *BCL2* expression should be considered for combination therapy with venetoclax.

KEY WORDS

AML, BET, BRD4, RUNX1, ETO, venetoclax, JQ1, AML1, metabolism

1 | INTRODUCTION

The bromodomain and extraterminal domain (BET) proteins consist of four family members including bromodomain-

containing protein 2 (BRD2), BRD3, BRD4, and BRDT.¹ These BET proteins bind to acetylated lysine in the tails of histones as well as other nonhistone nuclear proteins through two conserved N-terminal bromodomains.^{1–4} BET proteins are typically associated with enhancers and associate with positive transcription elongation factor b (P-TEFb) to

Susu Zhang and Yue Zhao are co-first authors.

regulate the transition from paused to elongating polymerase.⁵⁻⁸ In fact, the binding of BRD4 appears to release P-TEFb from the inhibitory HEXIM1-7SK complex.^{6,9,10} Small molecule inhibitors of BET proteins, such as JQ1, I-BET, and MS417 mimic the acetylated lysine moiety and competitively bind to the two bromodomains (BD1 and BD2) to displace BET proteins from chromatin.¹¹⁻¹³ JQ1 was originally identified as a tool compound to target midline carcinoma expressing a fusion protein caused by a chromosomal translocation between BRD4 and nuclear protein in testis (NUT).¹¹ However, BET inhibitors (BETi) also show efficacy in preclinical models of acute myeloid leukemia (AML), multiple myeloma, and certain types of lymphoma as well as other cancer types.^{8,11,14-19} RNA interference screening linked the inhibitory effect of these molecules to suppressing BRD4 activity in AML.¹⁵

Gene expression studies showed that BETi-induced downregulation of messenger RNAs including key oncogenes important for cell cycle progression, such as *MYC* and *E2F1* genes that control cell death such as *BCL2*, as well as lineage-specific oncogenes such as *BCL6*.^{8,11,14-16} Genomic binding studies revealed that these genes are associated with BRD4-enriched enhancers that are essential for the efficient transcription of these genes. The so-called “super-enhancers,” defined as clusters of subenhancers, are particularly sensitive to BETi, which rapidly displace BRD4 from chromatin causing the selective transcriptional repression of those super-enhancer–driven genes. However, as a global chromatin reader, BRD4 is also found at active promoters and typical enhancers. Moreover, inducible degradation of BRD4 indicated that it was a general factor that is required for the elongation of most expressed genes.²⁰

AML containing chromosomal translocations involving MLL appear to be especially sensitive to BETi,¹⁵ perhaps due to the translocations that fuse the N-terminal domain of MLL with components of the super elongation complex to stimulate the expression of key regulators of hematopoietic stem cell self-renewal such as Hox family members.²¹ Intriguingly, in these early studies, the t(8;21) cell line Kasumi-1 showed the most pronounced sensitivity.¹⁵ The t(8;21) is one of the most common chromosomal translocations in AML and fuses the N-terminal DNA binding domain of runt-related transcription factor 1 (RUNX1) to almost the entire eight-twenty-one (ETO) gene. While RUNX1 associates with multiple DNA binding proteins and/or histone modifying complexes to activate or repress transcription, the presence of the ETO moiety skews the activity of the fusion protein towards repression of RUNX1-regulated genes.²²⁻²⁵ That is, ETO can associate with histone acetyltransferases²⁶ but recruits class 1 histone deacetylases,²⁷ and global studies of t(8;21) cells suggest that this latter effect is the predominant mechanism of action.²⁸ However, ETO family members also associate with the “E proteins” HEB and Lyl1

in a complex containing LDB1, LMO2, and CDK9,^{29,30} leaving open the possibility that ETO family members regulate transcriptional elongation, which might explain the sensitivity of Kasumi-1 cells to BETi. By using precision nuclear run-on sequencing (PRO-seq), we previously identified many of the earliest targets of BET inhibitor action and demonstrated that these compounds cause transcriptional pausing of drivers of the cell cycle and metabolic activity, and affect enhancer RNA synthesis in the *MYC* super-enhancer.³¹ Here, we extended our study by showing that t(8;21) AML are not only highly sensitive to BETi but treatment with JQ1 or MS417 dramatically reduced cell size and induced cell cycle arrest rather than cell death. Cell cycle analyses and assessment of mitochondrial function and glycolytic activity indicated that the BETi-induced cell cycle arrest was reversible. However, the metabolic stress and impaired transcription of *BCL2* after JQ1 treatment provides further molecular rationale for combination therapy using BETi and venetoclax.

2 | MATERIALS AND METHODS

2.1 | Cell proliferation analysis

Cells were seeded at 2×10^5 cells/mL on the day of the experiment and treated with increasing doses of JQ1, MS417, or venetoclax for 3 consecutive days. Cell proliferation rate was measured on each day using alamarBlue assay (Thermo Fisher Scientific, Waltham, MA) according to the manufacturer’s instructions. Briefly, 100 μ L of cell suspension was transferred to a 96-well plate before 10 μ L of alamarBlue was added. Plates were incubated at 37°C for 4 hours, and alamarBlue fluorescence was measured at 590 nm. Viable cells were also quantified by Trypan Blue exclusion. Human primary AML cells were seeded at 5×10^5 cells/mL in a 96-well plate and treated with 250 nM JQ1 for 3 days. On day 3, alamarBlue was added and cells were incubated for 8 hours before reading.

2.2 | Assessment for cell size, cell cycle progression, and apoptosis

The distribution of cell size was analyzed using flow cytometry and presented using forward-scatter histogram plots. For cell cycle analyses, cells were treated with JQ1 or MS417 for 24, 48, and 72 hours, fixed with 70% ethanol in the cold room for overnight, and stained with propidium iodide (PI) at room temperature for 30 minutes before flow cytometry. For 5-bromo-2'-deoxyuridine (BrdU) analysis, 10 million cells were pulsed with 20 M BrdU for 1 hour and fixed with 70% ethanol in the cold room for overnight. Cells were stained with fluorescein isothiocyanate (FITC)-conjugated BrdU antibody

(556028; BD Biosciences, San Jose, CA) and counterstained with PI before analysis using flow cytometry. Apoptosis was analyzed using a FITC-annexin V/PI Apoptosis Detection Kit (556547; BD Pharmingen Biosciences, San Jose, CA). All flow cytometry figures were generated using FlowJo software (Ashland, OR).

2.3 | RNA sequencing

Poly A+ RNA (VANTAGE, Nashville, TN) and precision nuclear run-on sequencing reads were aligned to the human transcriptome hg19 (downloaded from the University of California, Santa Cruz [UCSC]) using Bowtie2 (version 2.2.4)³² and TopHat (version v2.0.10).³³

2.4 | Oxygen consumption rate and extracellular acidification rate measurements

Cells were seeded on Cell-Tak adhesive coated Seahorse XF96 Cell Culture Microplates to prepare adherent monolayer cultures. Seahorse XFe96 Extracellular flux analyzer (Agilent, Inc, Santa Clara, CA) was utilized to determine the oxygen consumption rate (OCR) and extracellular acidification rate (ECAR) by measuring the concentration of oxygen and free protons in the medium surrounding the monolayer of cells in real-time. The XF Cell Mito Stress Test Kit (Agilent, Inc., Santa Clara, CA) was used to access the mitochondrial function after serially injecting oligomycin, *p*-trifluoromethoxy carbonyl cyanide phenylhydrazine (FCCP), and a mix of rotenone and antimycin A to measure adenosine triphosphate (ATP) production, maximal respiration, and nonmitochondrial respiration, respectively. The XF Glycolysis Stress Test Kit (Agilent, Inc., Santa Clara, CA) was used to access the glycolysis capacity after three sequential injections of glucose, oligomycin, and 2-deoxyglucose.

2.5 | Optical metabolic imaging

Multiphoton fluorescence lifetime imaging was performed on a Nikon (Tokyo, Japan) Ti:E inverted microscope equipped with time-correlated single photon counting electronics. (NAD(P)H) and FAD fluorescence were excited with a titanium:sapphire laser (Chameleon Ultra II; Coherent, Inc (Santa Clara, CA)) tuned to 750 and 890 nm, respectively. A 400 to 480 nm bandpass filter was used to isolate NAD(P)H fluorescence emission, and a 500 nm high-pass dichroic mirror and 500 to 600 nm bandpass filter were used to isolate FAD fluorescence emission. Fluorescence signal was collected through a $\times 40$ oil-immersion objective across a $170 \times 170 \mu\text{m}$ field of view, capturing approximately 40 to 60 cells. Four fields of view

per sample were acquired, yielding 125 to 250 cells for each of three biological replicates. Images were processed with custom software previously described.³⁴ Briefly, the NAD(P) H and FAD intensities were calculated by integrating the fluorescence lifetime decay within each pixel. Then, the ratio of NAD(P)H intensity divided by FAD intensity (the optical redox ratio) was calculated at each pixel. Pixels within the cell cytoplasm were averaged and statistical differences were calculated on a per-cell level.

2.6 | Statistical analyses

For cell proliferation, apoptosis, and quantitative reverse-transcription polymerase chain reaction (RT-PCR) analyses, results were presented as mean \pm SEM for data following the normal distribution. Unpaired two-sided Student *t* test was used to compare the means between two independent treatments. For data that did not follow a normal distribution such as read density and pausing index analyses, the Wilcoxon signed-rank test was used for paired comparisons between two treatments. $P < 0.05$ were considered as statistically significant. Optical redox ratio was reported as mean \pm SEM for each condition. Mann-Whitney tests were used to compare optical redox ratio differences between control and treated samples.

3 | RESULTS

3.1 | BET inhibitors affect Kasumi-1 cell proliferation without inducing apoptosis

High throughput screens of cancer cell lines identified the t(8;21) cell line Kasumi-1 as the most sensitive cell type to the BETi JQ1 using alamarBlue assays as a surrogate for cell proliferation.¹⁵ Consistent with these previous studies, we found that Kasumi-1 cells, as well as the t(8;21)-containing SKNO-1 cell line that requires granulocyte-macrophage colony-stimulating factor (GM-CSF) for growth,³⁵ were more sensitive than MOLM13, and MV4-11 that contain MLL disruptions (Figure 1A) when using alamarBlue assays. However, alamarBlue measures metabolic output, rather than cell death. When we tested for cell death using JQ1 and another potent BET inhibitor, MS417,³⁶ which shares molecular and transcription targets with JQ1,³¹ both JQ1 and MS417 only had minor effects on triggering apoptosis in Kasumi-1 cells, whereas SKNO-1 showed more cell death at 48 hours (Figure 1B). In addition, while MOLM13 and MV4-11 cells required higher concentrations of BETi to show an effect in alamarBlue assays, MOLM13 cells showed minimal apoptosis, while BETi more robustly induced apoptosis in MV4-11 (Figure 1B).

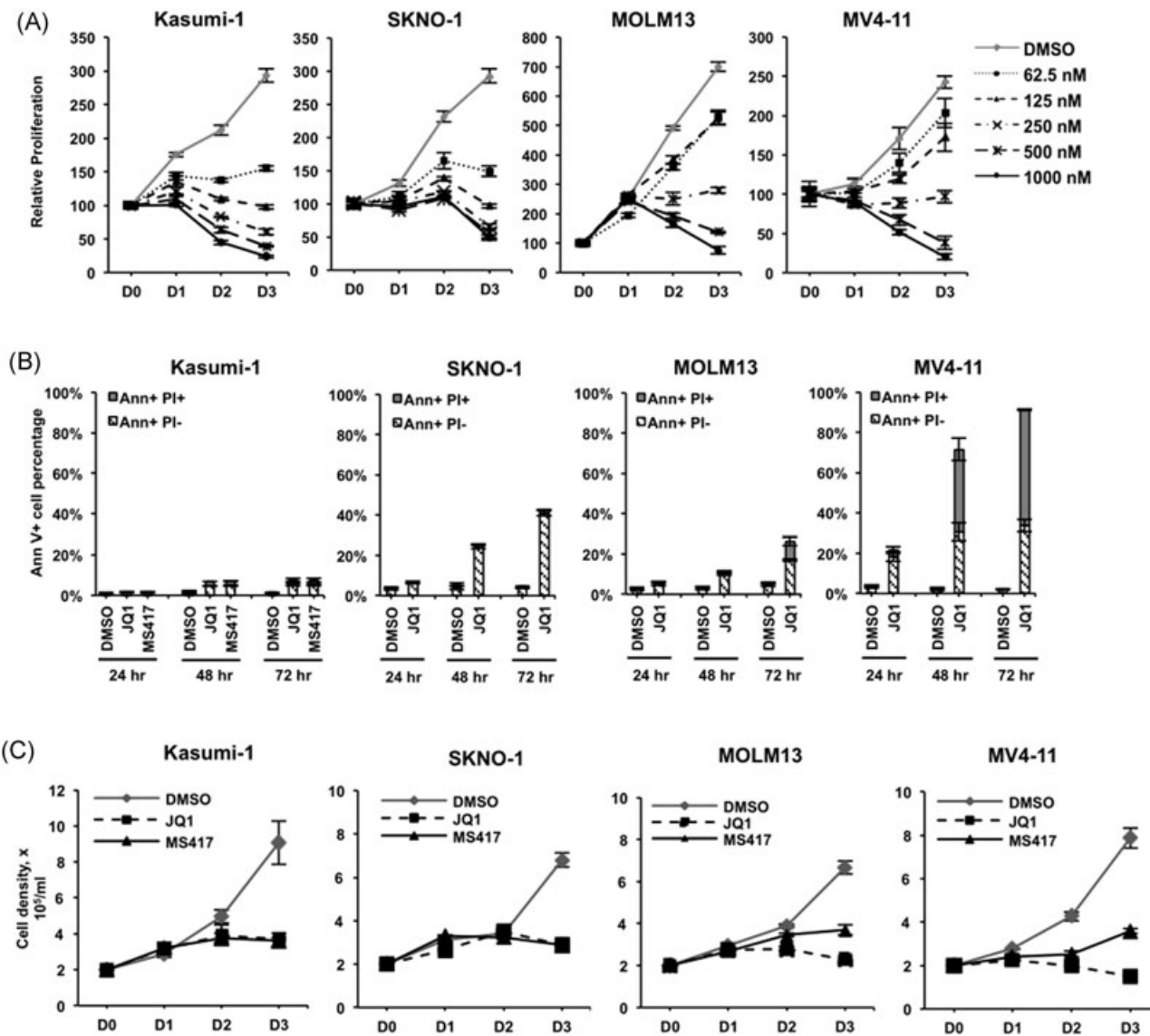


FIGURE 1 BETi inhibit proliferation but induce variable levels of cell death in AML cell lines. A, AlamarBlue assays show a dose-dependent loss of cellular metabolism after JQ1 treatment of Kasumi-1, SKNO-1, MOLM13, and MV4-11 cells for 3 days (D0-D3). Data are mean \pm SEM ($n = 3$). B, BETi induce variable levels of apoptosis. Kasumi-1 cells were treated with 250 nM JQ1 or 125 nM MS417. SKNO-1 were treated with 250 nM JQ1. MOLM13 and MV4-11 were treated with 500 nM JQ1. The levels of dying cells were quantified using AnnV+ and uptake of PI. Data are mean \pm SEM ($n = 4$). C, SKNO and Kasumi-1 cells were treated with 250 nM JQ1 or 125 nM MS417, whereas MOLM13 and MV4-11 were treated with twice these levels. Cell counts were determined using Trypan Blue dye exclusion. Data are mean \pm SEM ($n = 4$). AML, acute myeloid leukemia; AnnV+, annexin V positivity; BETi, bromodomain and extraterminal domain family; DMSO, dimethyl sulfoxide; PI, propidium iodide.

Consistent with these observations and in contrast to the alamarBlue data, manual cell viability counts using Trypan Blue dye exclusion showed JQ1 and MS417 had a cytostatic rather than cytotoxic effect on cell growth in Kasumi-1 cells but reduced the number of viable cells in cultures of MV4-11 cells (Figure 1C).

BETi disrupt the communication between enhancers and RNA polymerases that are paused just after transcriptional initiation. Inhibitors of P-TEFb (ie, CDK9 inhibitors), such as flavopiridol, also block RNA polymerase

elongation and cause DNA damage. However, we did not detect any phosphorylated H2AX in the nuclei of JQ1 or MS417 treated cells (Supporting Information Figure 1). This indicated that BETi inhibited cell proliferation without DNA double-strand breaks and without causing apoptosis in Kasumi-1 cells. Moreover, these compounds did not trigger a DNA damage-dependent cell cycle arrest or apoptosis of Kasumi-1 cells. These results raised the possibility that BETi directly or indirectly affected the metabolic rate as measured by alamarBlue.

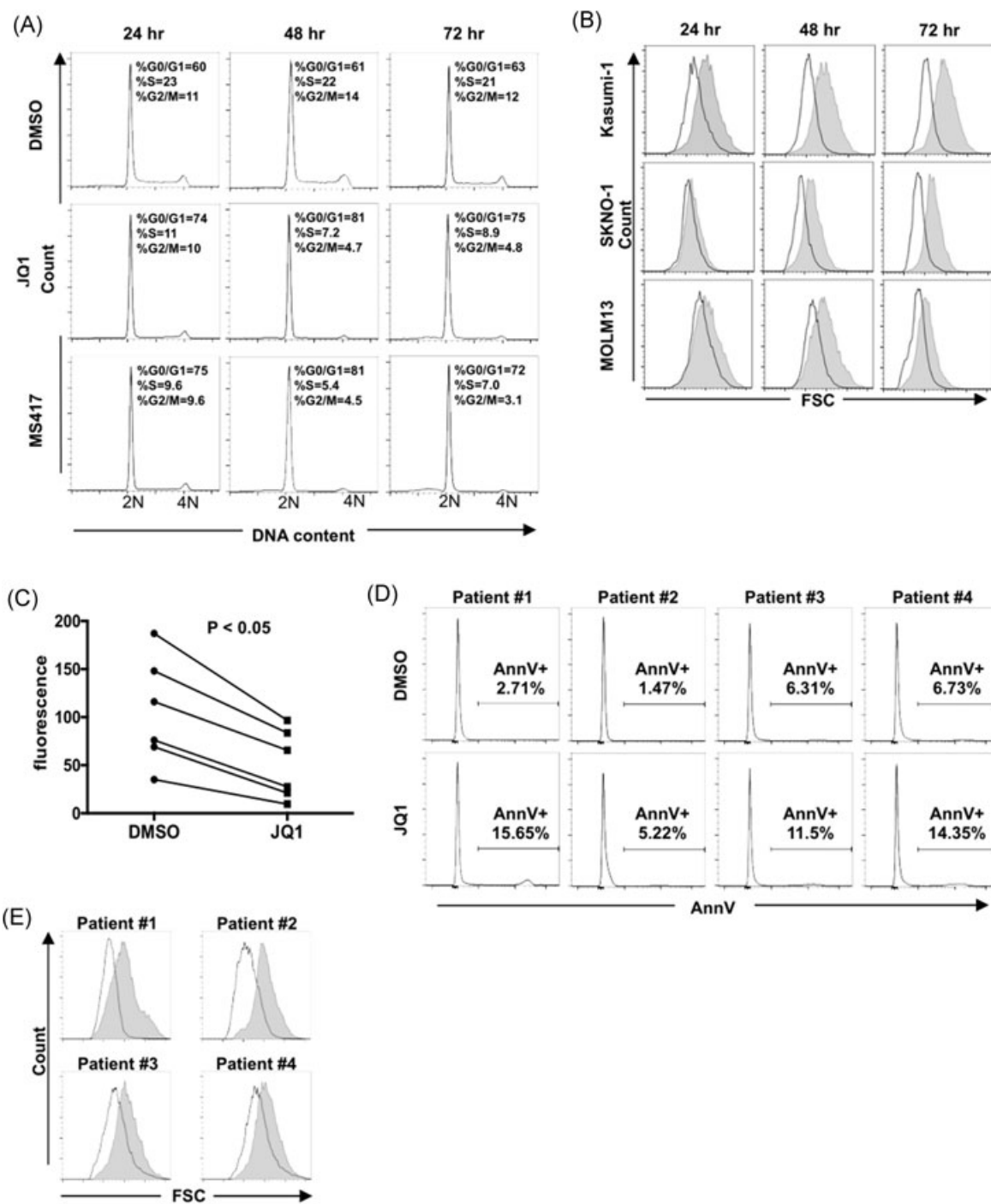


FIGURE 2 BETi induce cell cycle arrest and reduce cell size in t(8;21) AML cells. **A**, Cell cycle analyses of Kasumi-1 cells treated with BETi show cell cycle arrest with modest cell death 24 to 72 hours after treatment. Representative graphs of DNA content (2N to 4N) are shown ($n = 4$). **B**, Flow cytometry analyses showing forward scatter plots indicate that t(8;21) cells are distinctly smaller after treatment with 250 nM JQ1. Representative graphs are shown ($n = 4$). Shaded area represents DMSO and white plots represent JQ1. **C**, **D**, High blast count t(8;21) AML patient samples ($n = 6$) were treated with 250 nM JQ1 for 3 days. AlamarBlue assays show the inhibition of cell growth $P < 0.05$ by two-sided the Wilcoxon signed-rank test (C). **D**, Shows the lack of AnnV+ cells for four of the samples in C. **E**, Forward-scatter plots of flow cytometry analyses show that t(8;21) AML patient cells are distinctly smaller after JQ1 treatment of 3 days. Representative flow cytometry plots are shown. Shaded area represents DMSO and empty area represents JQ1. AML, acute myeloid leukemia; AnnV+, annexin V positivity; BETi, inhibitors of the bromodomain and extraterminal domain family; DMSO, dimethyl sulfoxide; FSC, forward scatter

3.2 | BET inhibitors reduce cell size

We extended this analysis using PI staining of DNA, which showed that Kasumi-1 cells treated with JQ1 and MS417 rapidly accumulated in the G₀/G₁ phase of the cell cycle (Figure 2A). Interestingly, we noted that treatment with BETi led to dramatic reductions in cell size in Kasumi-1 and SKNO-1 cells within 24 to 48 hours of treatment with JQ1, as assessed by diminished forward scatter in flow cytometry analysis (Figure 2B). JQ1 also reduced cell size in MOLM13 cells but the response was delayed (Figure 2B) relative to Kasumi-1 cells. While there were no apparent morphological changes toward

myeloid differentiation, Wright-Giemsa staining confirmed the smaller cell size and condensed nuclei of Kasumi-1 cells (Supporting Information Figure 2). Given the apparent sensitivity of t(8;21) cell lines, we extended this analysis to primary AML samples containing this translocation. Again, JQ1 inhibited cell growth as measured by alamarBlue staining without large increases in annexin V staining. These primary AML cells also showed a reduction in cell size (Figure 2C and 2E).

We further extended these observations to other leukemia/lymphoma cell lines, including Raji, K562, and MOLT4. JQ1 treatment reduced cell size in all cell lines tested (Figure 3A and 3D). This reduction in cell

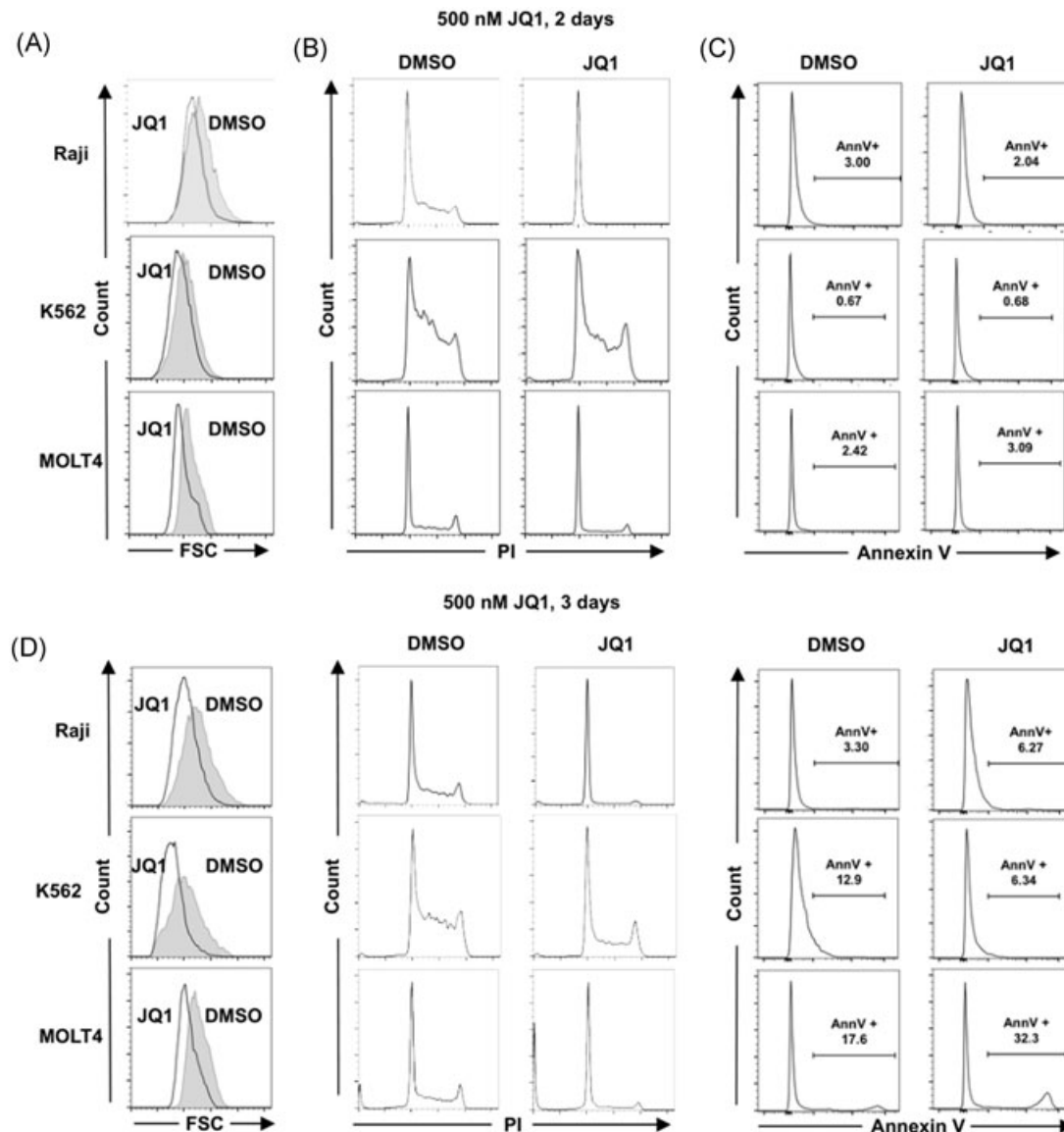


FIGURE 3 BETi reduces cell size in leukemia and lymphoma cell lines. A, Cell size was assessed using forward light scatter in flow cytometry. B, Cell cycle progression was assessed using propidium iodide staining. Representative graphs are shown. C, Apoptosis was assessed using annexin V positivity on viable cells. D, Similar analyses as in (A-C), but performed at day 3 with the indicated cell lines. Statistical analysis was performed as described in Figure 2. AML, acute myeloid leukemia; AnnV+, annexin V positivity; BETi, inhibitors of the bromodomain and extraterminal domain family; DMSO, dimethyl sulfoxide

size was associated with robust cell cycle arrest in all cell lines while the annexin V positive population was not greatly increased (Figure 3B and 3C) in the first 48 hours. Taken together, our data suggested that BET proteins are required for maintaining cell metabolism and cell size if the cells do not undergo rapid cell death.

3.3 | BET inhibitors reduce metabolic rate

The reduction in cell size is a classical phenotype associated with the loss of *MYC* expression and we observed a rapid loss of *MYC* transcription in Kasumi-1 cells treated with JQ1.³¹ Western blot analysis confirmed that *MYC* levels dropped within 2 hour in both Kasumi-1 cells and MV4-11 cells (Figure 4A). Therefore, we used pathway analysis tools to determine whether BET inhibitors affect the expression of

MYC targets and metabolic genes using our previously published PRO-seq data that were generated in Kasumi-1 cells treated with JQ1 or MS417 for 1 and 3 hours.³¹ PRO-seq provides a high-resolution map of the actively elongating RNA polymerases, which pinpoint the genes that are directly affected by small molecule inhibitors of transcription. Genes that were inhibited by both JQ1 and MS417 (generalized fold change [GFOLD] < -0.585) at 1 hour were enriched with signaling pathways mediated by cytokines and/or growth factors regulating cell proliferation that drive the accumulation of cell mass with progression through the cell cycle (Figure 4B). Genes inhibited at 3 hours were enriched in metabolic pathways and ribosome biogenesis (Figure 4B), which is consistent with reduced metabolism and cell size (Figures 1-3). *MYC* controls many of these metabolism-regulating genes and ribosomal genes to control cell size.³⁷⁻⁴¹ Gene set enrichment analysis (GSEA)

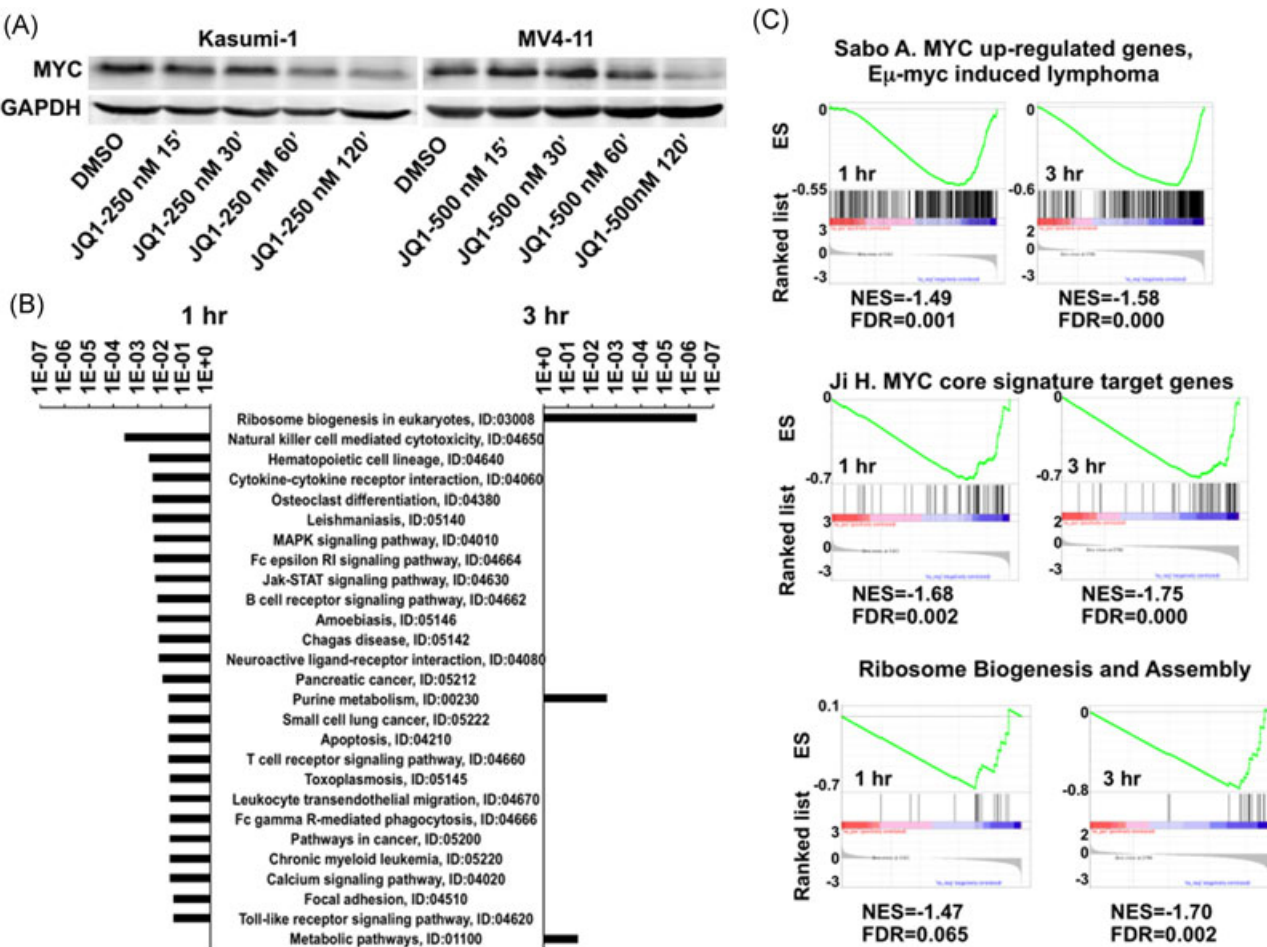


FIGURE 4 Meta-analysis of PRO-seq data of Kasumi-1 cells treated with JQ1 for 1 or 3 hours. A, MYC levels drop rapidly upon BETi treatment. Western blot analysis of Kasumi-1 (left panel) and MV4-11 (right panel) cells treated with 250 or 500 nM JQ1 for the indicated times. B, Kyoto Encyclopedia of Genes and Genomes pathway analysis of PRO-seq data³¹ showing genes in which promoter-proximal pausing was increased after 1 hour (left) and 3 hours (right) treatments. C, Gene set enrichment analysis of PRO-seq data³¹ showed decreased expression of MYC target genes including those genes regulating ribosomal biogenesis. BETi, inhibitors of the bromodomain and extraterminal domain family; DMSO, dimethyl sulfoxide; ES, enrichment score; FDR, false discovery rate; GAPDH, glyceraldehyde 3-phosphate dehydrogenase; NES, normalized enrichment score

supported this idea and showed that genes inhibited by BET inhibitors at both 1 and 3 hours were enriched with previously identified MYC target genes including genes regulating ribosomal biogenesis (Figure 4C).^{42–44} This suggests that BET inhibitors decrease the expression of genes regulating cell metabolism and cell size by impairing the transcription of MYC.

The role of BET inhibitors in reducing metabolism was further tested by directly examining bioenergetics in Kasumi-1, SKNO-1, and MOLM13 live cells by assessing the OCR and ECAR to track mitochondrial respiration and glycolysis using the Agilent Seahorse system (Figure 5). Cells were cultured in the absence or presence of BETi for 48 hours, and then assessed for 20 minutes to establish the basal respiration rates before injection of oligomycin to disrupt oxygen consumption and measure ATP production (Figure 5, top panel). BETi pretreatment reduced the basal respiration rate to essentially the level of control cells treated with oligomycin. Next, FCCP was injected to uncouple the respiratory chain from phosphorylation and assess the maximal respiration rates. BETi treated cells showed only a marginal response compared with a robust response from the untreated control cells. Finally, rotenone and antimycin A were injected to block respiration (Figure 5, top panel). Overall, JQ1 dramatically impaired mitochondrial functions.

Cancer cells reprogram their metabolic pathways and are more dependent on glycolysis as an energy source. Therefore, we assessed glycolytic activity in the absence or presence of JQ1 (Figure 5, bottom panels). Cells were again treated with JQ1 for 48 hours before a 15 minutes assessment of the basal nonglycolytic media acidification. Glucose was then injected to assess glycolysis followed by an injection of oligomycin 20 minutes later to impair ATP production. Untreated control cells showed a rapid burst of glycolytic activity upon addition of glucose, and oligomycin triggered a further increase in acidification indicating that control cells had a further glycolytic reserve (Figure 5, bottom panel). In contrast, JQ1-treated AML cells showed a poor glycolytic burst with no further increase in glycolytic capacity upon oligomycin injection (Figure 5, bottom panel).

3.4 | BET inhibitor-induced cell cycle arrest is reversible

The rapid onset of cell cycle arrest without apoptosis for the first 24 to 48 hours after continuous drug treatment suggested

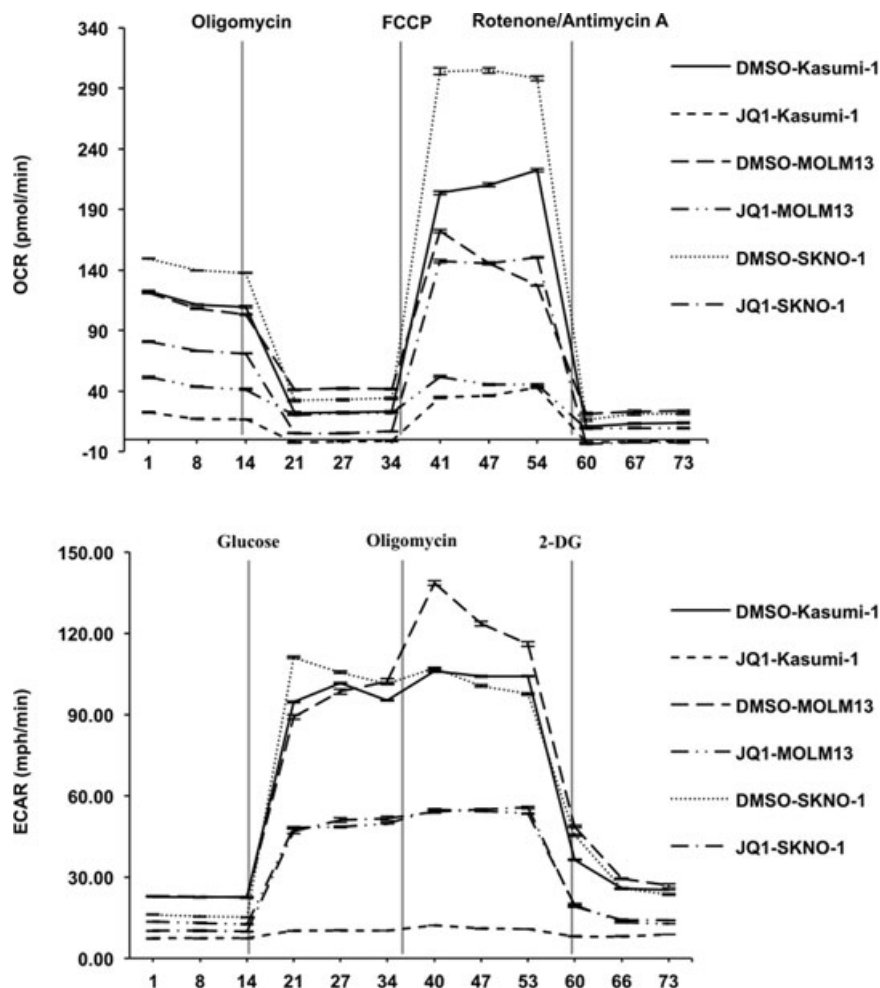


FIGURE 5 BET inhibitors reduce metabolic rate. OCR and ECAR were measured after JQ1 treatment of 2 days in Kasumi-1, MOLM13, and SKNO-1 cells. Decreased OCR and ECAR indicate repression of both mitochondrial dynamics and glycolytic function. For OCR, stage I injected oligomycin (5 mM), stage II injected FCCP (1 mM), and stage III injected rotenone/antimycin A (0.5 mM). For ECAR, stage I injected glucose (10 mM), stage II injected oligomycin (5 mM), and stage III injected 2-deoxyglucose (50 mM). ECAR, extracellular acidification rates; FCCP, *p*-trifluoromethoxy carbonyl cyanide phenylhydrazine; OCR, oxygen consumption rate

that even with daily dosing in patients the trough levels might allow survival of some AML cells.⁴⁵ To assess whether JQ1-treated cells still possessed proliferative potential after drug removal, which could ultimately cause leukemic cell repopulation and resistance to BET inhibitor therapy, we treated Kasumi-1 cells for 24, 48, or 72 hours, washed out the drug and then cultured them in fresh media and monitored cell growth. Consistent with these drugs inducing G₀/G₁ cell cycle arrest but not senescence or cell death, Kasumi-1 cells treated for 24 or 48 hours were rescued to some degree by removing the drug (Figure 6A, left and middle panels). However, longer treatments had a stronger effect on restricting cell proliferation as the cells treated for 3 days grew much slower during the first 3 days after drug removal (Figure 6A, right panel). The cells treated for 48 hours before rescue became more metabolically active 3 or 5 days after drug removal (Figure 6B, RD3 and RD5) and returned to normal size within 3 days after being transferred to fresh media (Figure 6C), and eventually began growing normally showing a rapid recovery of cell size and metabolism.

Next, we performed optical metabolic imaging using two-photon fluorescence imaging to measure the optical redox ratio of Kasumi-1 cells in response to JQ1 treatment and rescue. This approach captures intrinsic fluorescence of these coenzymes within live cells, and the optical redox ratio (NAD(P)H fluorescence intensity/FAD fluorescence intensity) informs on the relative oxidation or reduction state of the cells. This measurement distinguishes between apoptotic, proliferating, and G₀/G₁ cells.³⁴ JQ1-treated cells displayed a reduced redox ratio beginning at 24 hours after treatment, which was exacerbated by 72 hours (Figure 6D, left panel). Changes in redox ratio were reversed in response to recovering cells from JQ1 treatment, indicating negligible effects of apoptosis in this analysis (Figure 6D, right panel). Together, the combined effects of BET inhibitors on cell cycle arrest, cell size, and reduced metabolic rate suggested that the cells were not only being arrested in G₁ but were perhaps entering a G₀, quiescent-like, state.

Finally, we arrested cells with JQ1 for 72 hours (a time where the cells were beginning to die; Figure 1 and 2), washed the cells to remove the compound and cultured them in fresh media lacking JQ1 for 12 to 24 hours before quantifying the number of cells entering S phase using BrdU incorporation. By 12 hours after drug removal, cells were beginning to re-enter the early S phase and this trend continued through 24 hours (Figure 7A, JQ1 panels; Figure 7B, hashed bars). Intriguingly, it appears that some of the S phase-arrested cells began incorporating BrdU. Notably, cells already synthesizing DNA do not incorporate as much BrdU leading to a broadening of the band of cells in the 12, 18, and 24 hours samples (Figure 7A, JQ1 panels). Conversely, some cells with between 2 N and 4 N DNA content did not incorporate BrdU (Figure 7A, oval in the 0 hours panel),

suggesting that these cells were actually arrested in the S phase or were dying. Nevertheless, even after a 72 hours treatment with JQ1, there were cells that appeared to be quiescent but still capable of re-entering the cell cycle after drug removal, indicating a potential mechanism of resistance to BETi.

3.5 | BET inhibitors sensitize cells to BCL2 inhibitors

The finding that BET inhibitors can arrest the cell cycle without dramatic AML cell killing suggested the need for combination therapy. The antiapoptotic protein BCL2 is often expressed in leukemia cells and our earlier study showed that BET inhibitors caused promoter-proximal pausing of RNA polymerase II and reduced the rate of transcription of *BCL2* and *BCL-xL* in Kasumi-1 cells.³¹ Therefore, we tested the combination of BET inhibitor and BCL2 inhibitors to target the residual BCL2. We pretreated Kasumi-1 cells with JQ1 for 2 days to downregulate the expression of *BCL2* and *BCL-xL* and found that the addition of BCL2/BCL-xL (ABT-263) or BCL2-selective (venetoclax [ABT-199]) inhibitors quickly triggered apoptosis as measured by annexin V and PI staining (Figure 8A). We next extended this cotreatment analysis to other cell lines (SKNO-1, MOLM13, and MOLT4) that also showed cell cycle arrest with little apoptosis (Figures 1-3) and found that inhibiting BCL2 family proteins following BET inhibitor pretreatment also induced cell death (Figure 8B to 8D). This suggests that entering a reversible cell cycle arrest induced by BET inhibitors may protect leukemia cells from rapid cell death and increase the chance of relapse, which necessitates a second drug (eg, BCL2 inhibitor) to induce cell death for the efficient killing of leukemia cells.

4 | DISCUSSION

While there is justifiable excitement about the therapeutic efficacy of BETi in AML, the therapeutic window appears to be due to the loss of MYC expression.^{8,11,14-16,18} However, as observed in Kasumi-1 cells, the rapid loss of MYC was accompanied by a rapid cell cycle arrest, loss of metabolic activity, and reduced cell size, which is reminiscent of quiescence rather than cell death. In standard assays that use metabolism as a surrogate marker for cell viability, these compounds appear to work well, yet these cells recovered after BETi removal, suggesting that cell cycle arrest could be a mechanism of resistance to these compounds. The addition of a BCL2 inhibitor could provide the additional push toward apoptosis needed and this could be an extremely safe and efficacious combination.

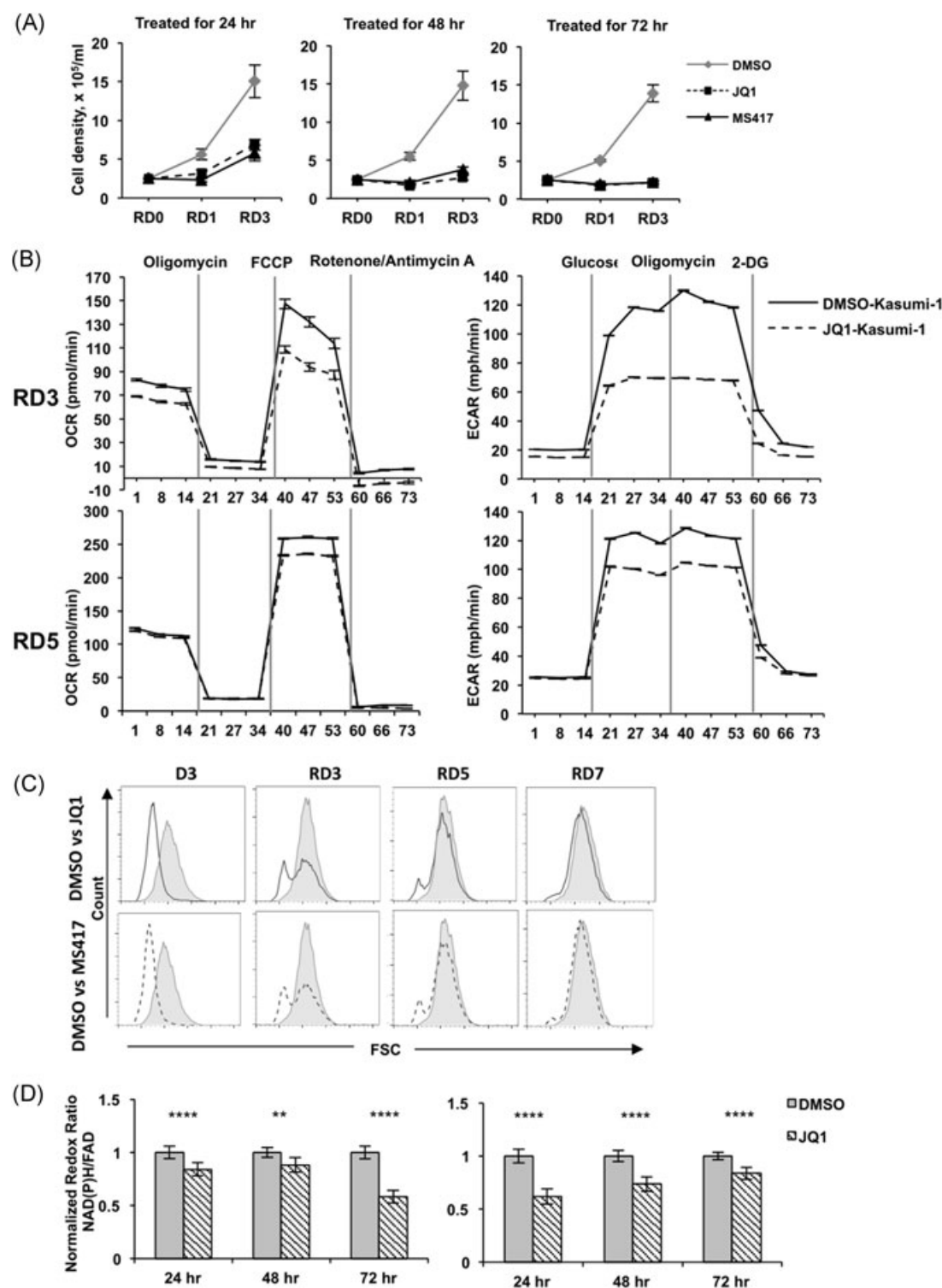


FIGURE 6 Metabolic effects of BETi are reversible. A, Kasumi-1 cells were treated with BETi for 24, 48, or 72 hours and the cells allowed to recover for 0, 1, or 3 days. Viable cell numbers were graphed over time. B, OCR and ECAR were measured after treatment of Kasumi-1 cells for 2 days and allowed to recover in the absence of JQ1 for 3 or 5 days. For OCR, stage I injected oligomycin (5 mM), stage II injected FCCP (1 mM), and stage III injected rotenone/antimycin A (0.5 mM). For ECAR, stage I injected glucose (10 mM), stage II injected oligomycin (5 mM), and stage III injected 2-deoxyglucose (50 mM). C, Kasumi-1 cells treated with BETi for 3 days (D3) and then allowed to recover for 3, 5, or 7 days without BETi were tested for cell size using forward scatter in FACS. D, Normalized optical redox ratio (NAD(P)H/FAD) was assessed using optical metabolic imaging. A minimum of 125 cells per sample in biological triplicates were measured for DMSO- and JQ1-treated Kasumi-1 cells at 24 to 72 hours before washout (left panel) or for the 24 to 72 hours after washout (recovery) of JQ1 (right panel). ** $P < 0.01$ and *** $P < 0.0001$; Mann-Whitney test. BETi, inhibitors of the bromodomain and extraterminal domain family; DMSO, dimethyl sulfoxide; ECAR, extracellular acidification rates; FACS, fluorescence-activated cell sorting; FCCP, *p*-trifluoromethoxy carbonyl cyanide phenylhydrazine; OCR, oxygen consumption rate

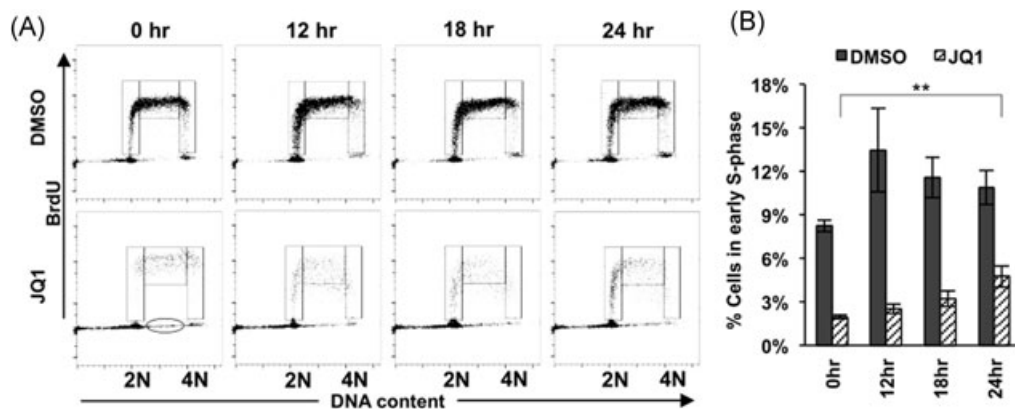


FIGURE 7 BETi induce reversible cell cycle arrest in Kasumi-1 cells. A, Flow cytometry plots of incorporated BrdU versus propidium iodide show that Kasumi-1 cells treated with 250 nM JQ1 for 72 hours can recover and re-enter the cell cycle after drug removal for the indicated times. Cells were gated as early, middle, and late S phases from left to right. Oval indicates BrdU⁻ cells in the S phase. B, Bar graph displays the percentage of cells in the early the S phase. Data are presented as mean \pm SEM ($n = 4$). ** $P < 0.001$ by two-sided Student *t* test when 0 and 24 hours levels were compared. BETi, inhibitors of the bromodomain and extraterminal domain family; BrdU, 5-bromo-2'-deoxyuridine; DMSO, dimethyl sulfoxide

We identified this effect in t(8;21) containing Kasumi-1 cells, yet the effect was not limited to the t(8;21), as cells that express MLL fusion proteins were similarly slow to die in response to BETi. In addition, in a panel of diffuse large B-cell lymphoma cell lines, JQ1 strongly induced G₁ cell cycle arrest but only caused minor levels of apoptosis in several of these cell types (eg, Ly7, Toledo, and Ly19).⁸ Poor pharmacokinetic profile has been proposed as the cause of the greatly reduced efficacy of BETi in mouse models compared with in vitro studies with cell lines but reversible cell cycle arrest likely contributes. This may be a limiting factor for the usefulness of these compounds as *MYC* activation is a later event in myeloid leukemias that are not triggered by a translocation or amplification directly affecting *MYC*. This is an important consideration because when additional oncogenes together with *MYC* drove AML development, removal of *MYC* expression failed to prevent tumor recurrence.^{46,47}

Mechanistically, *MYC* is perhaps the best known transcriptional regulator of metabolism, cell cycle, and cell size,⁴⁸ as it controls the production of ribosomes that control translational outputs. Thus, it is most likely that suppression of *MYC* is the key event in the regulation of cell size in our studies. It is notable that our PRO-seq analysis did not identify RNA polymerase II promoter-proximal pausing associated with ribosomal genes or pathways linked to metabolism until 3 hours after JQ1 treatment (Figure 4A), even though large numbers of genes were affected within 15 to 30 minutes after treatment, including *MYC*.³¹ Thus, the loss of metabolic activity (Figures 5 and 6) is likely a secondary consequence, which is consistent with the down-regulation of *MYC* in the first hour followed by the loss of *MYC* targets beginning at 1 hour and increasing 3 hours post

drug treatment (Figure 4). However, we also noted the loss of expression of cyclin D1 (*CCND1*) and D2 (*CCND2*), CDK4, and CDK6. In addition, we detected an “E2F/retinoblastoma (RB) signature” of increased pausing ratio with E2F2 and E2F8 being directly affected within the first hour of treatment with BETi.³¹ Conversely, we noted a rapid upregulation of *CDKN1A* (*p21^{CIP}*) but this was not associated with DNA damage (Supporting Information Figure S1). Given that RB family-dependent repression is associated with G₁ arrest and quiescence and E2F family members control nucleotide metabolism, these data suggest that the effects on metabolism and cell cycle control are multifactorial in nature.

In addition to controlling cell size, *MYC* is a direct regulator of genes that control glycolysis and mitochondrial biogenesis (Figures 5 and 6).⁴⁹ *MYC* stimulates the expression of glucose transporter-1 while also stimulating the genes that directly control glycolysis.⁵⁰⁻⁵² Therefore, the loss of *MYC* expression is consistent with the loss of glycolytic burst and glycolytic capacity in AML cells treated with JQ1 (Figure 5). At the same time, JQ1 treatment induced a loss of mitochondrial functions including reductions in basal respiration, ATP-linked respiration, and maximal respiration capacity (Figure 5). Analysis of transcription at the early time points suggested only defects in growth factor signal transduction, so these effects could also be traced to reduced *MYC* expression by three hours post BET inhibitor treatment.

Given the loss of *MYC* expression and the large effects on metabolism, it is somewhat surprising that AML cells survived and could re-enter the cell cycle (Figures 6 and 7). An intriguing hypothesis is that the cells have entered a quiescent-like state in which metabolic needs are greatly

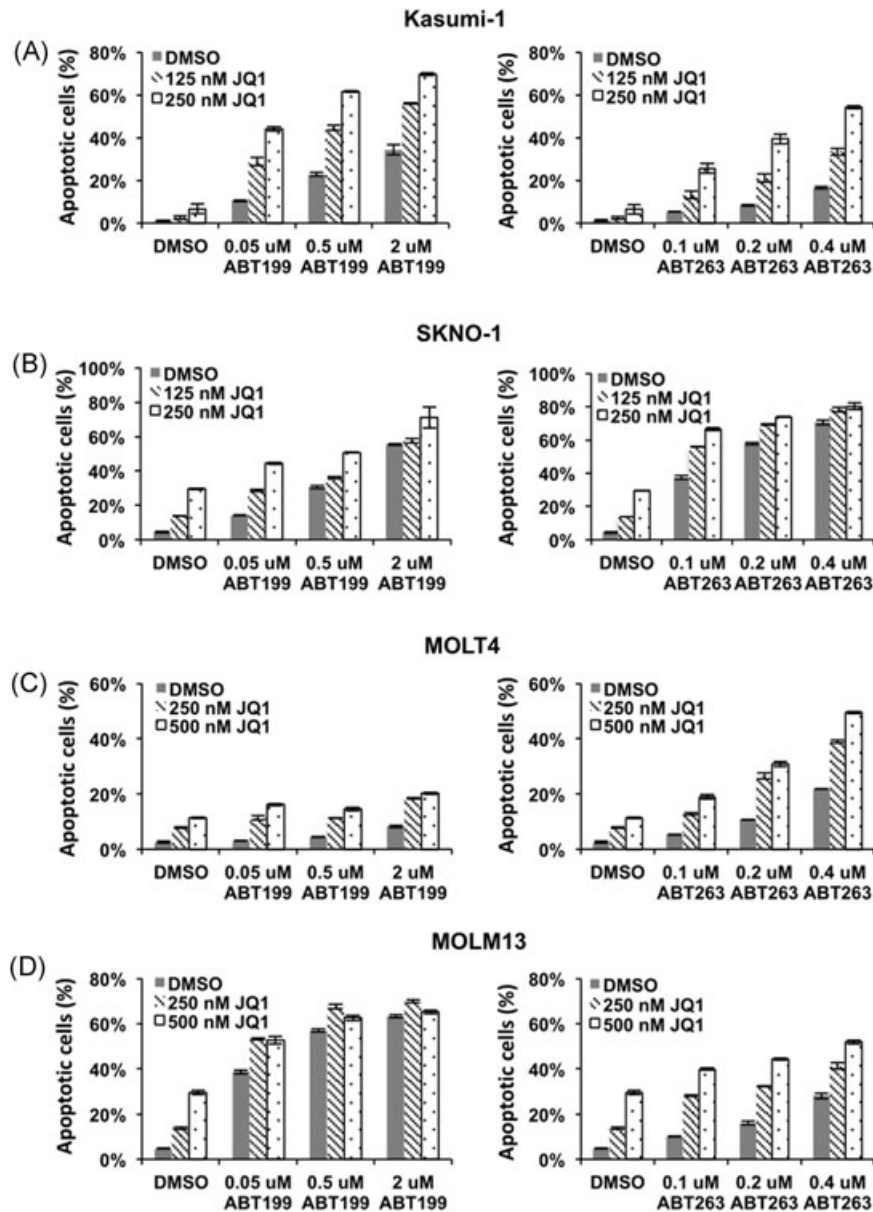


FIGURE 8 BET inhibitors sensitize AML cells to BCL2 inhibitor-induced cell death. AML cell lines were treated with BCL2-selective (ABT-199) or BCL2/BCL-xL (ABT-263) inhibitors for 6 hours after pretreating with BETi for 2 days. Apoptotic cell population was detected by annexin V positivity and the absence of propidium iodide staining. Data are mean \pm SEM ($n = 3$). A, Kasumi-1 cells and (B) SKNO-1 cells were incubated with 125 or 250 nM JQ1 before BCL2 inhibitor treatment. C, MOLT4 cells and (D) MOLM13 cells were incubated with 250 or 500 nM JQ1 before BCL2 inhibitor treatment. AML, acute myeloid leukemia; BET, bromodomain and extraterminal domain; DMSO, dimethyl sulfoxide

reduced. This possibility is consistent with the gene expression profiles, the reduced cell size and the ability of these cells to begin cycling again after removal of JQ1. Nevertheless, the increased apoptosis upon addition of venetoclax was more than an additive effect in Kasumi-1 cells indicating that the suppression of BCL2 levels sets the stage for the induction of apoptosis. While the effects were not as dramatic in other cell types (Figure 8), this could be due to induction of MCL1, whose levels increase after JQ1 treatment, possibly as a stress response. Given that venetoclax is beginning to gain traction as a component of the standard of care for AML,^{53–56} these data support a rational combination approach to the utilization of BET inhibitors with venetoclax in the clinic to avoid the use of genotoxic agents such as hypomethylating agents or Cytarabine.

ACKNOWLEDGMENTS

We thank all the members of Hiebert Laboratory for helpful discussions, reagents, and advice. We thank the translational pathology, the hematological sample repository, flow cytometry, and VANTAGE Shared Resources for services and support. This study was supported by the T. J. Martell Foundation, the Robert J. Kleberg, Jr. and Helen C. Kleberg Foundation, National Institutes of Health (grants, RO1-CA109355, RO1-CA164605, and RO1-CA64140) and core services performed through Vanderbilt Digestive Disease Research Center (grant, NIDDK P30DK58404) and the Vanderbilt-Ingram Cancer Center support (grant, NCI P30CA68485). KS was supported by 5 T32 CA009582-31 and a postdoctoral fellowship (PF-13-303-01-DMC) from the American Cancer Society. The project described was also

supported by the National Center for Research Resources (grant, UL1 RR024975-01) and is now at the National Center for Advancing Translational Sciences (grant, 2 UL1 TR000445-06). This study was supported by grant 1S10OD018015-01A1 for the Seahorse Extracellular Flux Analyzer and Prep Station, housed in the Vanderbilt High-Throughput Screening Facility. The content is solely the responsibility of the authors and does not necessarily represent the official views of the National Institutes of Health (NIH). Dr. Savona receives grants, personal fees and non-financial support from Astex, Boehringer-Ingelheim, Celgene Karyopharm, Sunesis, Takeda, TG Therapeutics, Gilead, and Incyte Corporation that are unrelated to this work. Dr. Hiebert receives grants and personal fees from Incyte Corporation that are unrelated to this work.

ORCID

Scott W. Hiebert  <http://orcid.org/0000-0001-5621-1454>

REFERENCES

- Wu SY, Chiang CM. The double bromodomain-containing chromatin adaptor Brd4 and transcriptional regulation. *J Biol Chem*. 2007;282:13141-13145.
- Dey A, Chitsaz F, Abbasi A, Misteli T, Ozato K. The double bromodomain protein Brd4 binds to acetylated chromatin during interphase and mitosis. *Proc Natl Acad Sci USA*. 2003;100:8758-8763.
- Filippakopoulos P, Knapp S. The bromodomain interaction module. *FEBS Lett*. 2012;586:2692-2704.
- Zhang G, Plotnikov AN, Rusinova E, Shen T, Morohashi K, Joshua J, et al. Structure-guided design of potent diazobenzene inhibitors for the BET bromodomains. *J Med Chem*. 2013;56:9251-9264.
- Jang MK, Mochizuki K, Zhou M, Jeong HS, Brady JN, Ozato K. The bromodomain protein Brd4 is a positive regulatory component of P-TEFb and stimulates RNA polymerase II-dependent transcription. *Mol Cell*. 2005;19:523-534.
- Yang Z, Yik JHN, Chen R, He N, Jang MK, Ozato K, et al. Recruitment of P-TEFb for stimulation of transcriptional elongation by the bromodomain protein Brd4. *Mol Cell*. 2005;19:535-545.
- Lovén J, Hoke HA, Lin CY, Lau A, Orlando DA, Vakoc CR, et al. Selective inhibition of tumor oncogenes by disruption of super-enhancers. *Cell*. 2013;153:320-334.
- Chapuy B, McKeown MR, Lin CY, Monti S, Roemer MGM, Qi J, et al. Discovery and characterization of super-enhancer-associated dependencies in diffuse large B cell lymphoma. *Cancer Cell*. 2013;24:777-90.
- Bartholomeeusen K, Xiang Y, Fujinaga K, Peterlin BM. Bromodomain and extraterminal (BET) bromodomain inhibition activate transcription via transient release of positive transcription elongation factor b (P-TEFb) from 7SK small nuclear ribonucleoprotein. *J Biol Chem*. 2012;287:36609-36616.
- Liu L, Xu Y, He M, Zhang M, Cui F, Lu L, et al. Transcriptional pause release is a rate-limiting step for somatic cell reprogramming. *Cell Stem Cell*. 2014;15:574-588.
- Filippakopoulos P, Qi J, Picaud S, Shen Y, Smith WB, Fedorov O, et al. Selective inhibition of BET bromodomains. *Nature*. 2010;468:1067-1073.
- Nicodeme E, Jeffrey KL, Schaefer U, Beinke S, Dewell S, Chung C, et al. Suppression of inflammation by a synthetic histone mimic. *Nature*. 2010;468:1119-1123.
- Zhang W, Prakash C, Sum C, Gong Y, Li Y, Kwok JJJ, et al. Bromodomain-containing protein 4 (BRD4) regulates RNA polymerase II serine 2 phosphorylation in human CD4⁺ T cells. *J Biol Chem*. 2012;287:43137-43155.
- Delmore JE, Issa GC, Lemieux ME, Rahl PB, Shi J, Jacobs HM, et al. BET bromodomain inhibition as a therapeutic strategy to target c-Myc. *Cell*. 2011;146:904-917.
- Zuber J, Shi J, Wang E, Rappaport AR, Herrmann H, Sison EA, et al. RNAi screen identifies Brd4 as a therapeutic target in acute myeloid leukaemia. *Nature*. 2011;478:524-528.
- Ott CJ, Kopp N, Bird L, Paranal RM, Qi J, Bowman T, et al. BET bromodomain inhibition targets both c-MYC and IL7R in high-risk acute lymphoblastic leukemia. *Blood*. 2012;120:2843-2852.
- Dawson MA, Prinjha RK, Dittmann A, Girotopoulos G, Bantscheff M, Chan WI, et al. Inhibition of BET recruitment to chromatin as an effective treatment for MLL-fusion leukaemia. *Nature*. 2011;478:529-533.
- Lockwood WW, Zejnnullahu K, Bradner JE, Varmus H. Sensitivity of human lung adenocarcinoma cell lines to targeted inhibition of BET epigenetic signaling proteins. *Proc Natl Acad Sci USA*. 2012;109:19408-19413.
- Feng Q, Zhang Z, Shea MJ, Creighton CJ, Coarfa C, Hilsenbeck SG, et al. An epigenomic approach to therapy for tamoxifen-resistant breast cancer. *Cell Res*. 2014;24:809-819.
- Winter GE, Mayer A, Buckley DL, Erb MA, Roderick JE, Vittori S, et al. BET bromodomain proteins function as master transcription elongation factors independent of CDK9 recruitment. *Mol Cell*. 2017;67:5-18.
- Mohan M, Lin C, Guest E, Shilatifard A. Licensed to elongate: a molecular mechanism for MLL-based leukaemogenesis. *Nat Rev Cancer*. 2010;10:721-728.
- Meyers S, Lenny N, Hiebert SW. The t(8;21) fusion protein interferes with AML-1B-dependent transcriptional activation. *Mol Cell Biol*. 1995;15:1974-1982.
- Lutterbach B, Sun D, Schuetz J, Hiebert SW. The MYND motif is required for repression of basal transcription from the multidrug resistance-1 promoter by the t(8;21) fusion protein. *Mol Cell Biol*. 1998;18:3601-3611.
- Lutterbach B, Westendorf JJ, Linggi B, Patten A, Moniwa M, Davie JR, et al. ETO, a target of t(8;21) in acute leukemia, interacts with the N-CoR and mSin3 corepressors. *Mol Cell Biol*. 1998;18:7176-7184.
- Linggi B, Müller-Tidow C, van de Locht L, Hu M, Nip J, Serve H, et al. The t(8;21) fusion protein, AML1 ETO, specifically represses the transcription of the p14(ARF) tumor suppressor in acute myeloid leukemia. *Nat Med*. 2002;8:743-750.
- Wang L, Gural A, Sun XJ, Zhao X, Perna F, Huang G, et al. The leukemogenicity of AML1-ETO is dependent on site-specific lysine acetylation. *Science*. 2011;333:765-769.

27. Amann JM, Nip J, Strom DK, Lutterbach B, Harada H, Lenny N, et al. ETO, a target of t(8;21) in acute leukemia, makes distinct contacts with multiple histone deacetylases and binds mSin3A through its oligomerization domain. *Mol Cell Biol*. 2001;21:6470-6483.
28. Ptasinska A, Assi SA, Martinez-Soria N, Imperato MR, Piper J, Cauchy P, et al. Identification of a dynamic core transcriptional network in t(8;21) AML that regulates differentiation block and self-renewal. *Cell Rep*. 2014;8:1974-1988.
29. Zhang J, Kalkum M, Yamamura S, Chait BT, Roeder RG. E protein silencing by the leukemogenic AML1-ETO fusion protein. *Science*. 2004;305:1286-1289.
30. Meier N, Krpic S, Rodriguez P, Strouboulis J, Monti M, Krijgsveld J, et al. Novel binding partners of Ldb1 are required for hematopoietic development. *Development*. 2006;133:4913-4923.
31. Zhao Y, Liu Q, Acharya P, Stengel KR, Sheng Q, Zhou X, et al. High-resolution mapping of RNA polymerases identifies mechanisms of sensitivity and resistance to BET inhibitors in t(8;21) AML. *Cell Rep*. 2016;16:2003-2016.
32. Langmead B, Salzberg SL. Fast gapped-read alignment with Bowtie 2. *Nat Methods*. 2012;9:357-359.
33. Kim D, Pertea G, Trapnell C, Pimentel H, Kelley R, Salzberg SL. TopHat2: accurate alignment of transcriptomes in the presence of insertions, deletions and gene fusions. *Genome Biol*. 2013;14:R36.
34. Heaster TM, Walsh AJ, Zhao Y, Hiebert SW, Skala MC. Autofluorescence imaging identifies tumor cell-cycle status on a single-cell level. *J Biophotonics*. 2018;11:e201600276.
35. Matozaki S, Nakagawa T, Kawaguchi R, Aozaki R, Tsutsumi M, Murayama T, et al. Establishment of a myeloid leukaemic cell line (SKNO-1) from a patient with t(8;21) who acquired monosomy 17 during disease progression. *Br J Haematol*. 1995;89:805-811.
36. Zhang G, Liu R, Zhong Y, Plotnikov AN, Zhang W, Zeng L, et al. Downregulation of NF-kappaB transcriptional activity in HIV-associated kidney disease by BRD4 inhibition. *J Biol Chem*. 2012;287:28840-28851.
37. Mateyak MK, Obaya AJ, Adachi S, Sedivy JM. Phenotypes of c-Myc-deficient rat fibroblasts isolated by targeted homologous recombination. *Cell Growth Differ*. 1997;8:1039-1048.
38. Mateyak MK, Obaya AJ, Sedivy JM. c-Myc regulates cyclin D-Cdk4 and -Cdk6 activity but affects cell cycle progression at multiple independent points. *Mol Cell Biol*. 1999;19:4672-4683.
39. Graves JA, Wang Y, Sims-Lucas S, Cherok E, Rothermund K, Branca MF, et al. Mitochondrial structure, function, and dynamics are temporally controlled by c-Myc. *PLOS One*. 2012;7:e37699.
40. Grewal SS, Li L, Orian A, Eisenman RN, Edgar BA. Myc-dependent regulation of ribosomal RNA synthesis during drosophila development. *Nat Cell Biol*. 2005;7:295-302.
41. Boon K, Caron HN, van Asperen R, Valentijn L, Hermus MC, van Sluis P, et al. N-myc enhances the expression of a large set of genes functioning in ribosome biogenesis and protein synthesis. *EMBO J*. 2001;20:1383-1393.
42. Ji H, Wu G, Zhan X, Nolan A, Koh C, De Marzo A, et al. Cell-type independent MYC target genes reveal a primordial signature involved in biomass accumulation. *PLOS One*. 2011;6:e26057.
43. Sabò A, Kress TR, Pelizzola M, de Pretis S, Gorski MM, Tesi A, et al. Selective transcriptional regulation by Myc in cellular growth control and lymphomagenesis. *Nature*. 2014;511:488-492.
44. Walz S, Lorenzin F, Morton J, Wiese KE, von Eyss B, Herold S, et al. Activation and repression by oncogenic MYC shape tumour-specific gene expression profiles. *Nature*. 2014;511:483-487.
45. Odore E, Lokiec F, Cvitkovic E, Bekradda M, Herait P, Bourdel F, et al. Phase I population pharmacokinetic assessment of the oral bromodomain inhibitor OTX015 in patients with haematologic malignancies. *Clin Pharmacokinet*. 2016;55:397-405.
46. Rakhra K, Bachireddy P, Zubuawala T, Zeiser R, Xu L, Kopelman A, et al. CD4(+) T cells contribute to the remodeling of the microenvironment required for sustained tumor regression upon oncogene inactivation. *Cancer Cell*. 2010;18:485-498.
47. Choi PS, Li Y, Felsher DW. Addiction to multiple oncogenes can be exploited to prevent the emergence of therapeutic resistance. *Proc Natl Acad Sci USA*. 2014;111:E3316-E3324.
48. Van Riggelen J, Yetil A, Felsher DW. MYC as a regulator of ribosome biogenesis and protein synthesis. *Nat Rev Cancer*. 2010;10:301-309.
49. Dang CV. A time for MYC: metabolism and therapy. *Cold Spring Harb Symp Quant Biol*. 2016;81:79-83.
50. Osthus RC, Shim H, Kim S, Li Q, Reddy R, Mukherjee M, et al. Dereulation of glucose transporter 1 and glycolytic gene expression by c-Myc. *J Biol Chem*. 2000;275:21797-21800.
51. Kim J, Zeller KI, Wang Y, Jegga AG, Aronow BJ, O'Donnell KA, et al. Evaluation of myc E-box phylogenetic footprints in glycolytic genes by chromatin immunoprecipitation assays. *Mol Cell Biol*. 2004;24:5923-5936.
52. Hu S, Balakrishnan A, Bok RA, Anderton B, Larson PEZ, Nelson SJ, et al. 13C-pyruvate imaging reveals alterations in glycolysis that precede c-Myc-induced tumor formation and regression. *Cell Metab*. 2011;14:131-142.
53. DiNardo CD, Pratz KW, Letai A, Jonas BA, Wei AH, Thirman M, et al. Safety and preliminary efficacy of venetoclax with decitabine or azacitidine in elderly patients with previously untreated acute myeloid leukaemia: a non-randomised, open-label, phase 1b study. *Lancet Oncol*. 2018;19:216-228.
54. Konopleva M, Letai A. BCL-2 inhibition in AML—an unexpected bonus? *Blood*. 2018;132:1007-1012.
55. Konopleva M, Polley DA, Potluri J, Chyla B, Hogdal L, Busman T, et al. Efficacy and biological correlates of response in a phase II study of venetoclax monotherapy in patients with acute myelogenous leukemia. *Cancer Discov*. 2016;6:1106-1117.
56. Sharma P, Polley DA. Shutting down acute myeloid leukemia and myelodysplastic syndrome with BCL-2 family protein inhibition. *Curr Hematol Malig Rep*. 2018;13:256-264.

SUPPORTING INFORMATION

Additional supporting information may be found online in the Supporting Information section at the end of the article.

How to cite this article: Zhang S, Zhao Y, Heaster TM, et al. BET inhibitors reduce cell size and induce reversible cell cycle arrest in AML. *J Cell Biochem*. 2018;114.
<https://doi.org/10.1002/jcb.28005>